Published in: 2016 IEEE 84th Vehicular Technology Conference (VTC-Fall)
DOI: 10.1109/VTCFall.2016.7880932

Client-Based Control Channel Analysis for Connectivity Estimation in LTE Networks

Robert Falkenberg, Christoph Ide and Christian Wietfeld
Communication Networks Institute
TU Dortmund University
44227 Dortmund, Germany
Email: {Robert.Falkenberg, Christoph.Ide, Christian.Wietfeld}@tu-dortmund.de

***Abstract*—Advanced Cyber-Physical Systems aim for the balancing of restricted local resources of deeply embedded systems with cloud-based resources depending on the availability of network connectivity: in case of excellent connectivity, the offloading of large amounts of data can be more efficient than the local processing on a resource-constraint platform, while this latter solution is preferred in case of limited connectivity. This paper proposes a Client-Based Control Channel Analysis for Connectivity Estimation (C^{3}ACE), a new passive probing mechanism to enable the client-side to estimate the connection quality of 4G networks in range. The results show that by observing and analyzing the control traffic in real-time, the number of active user equipment in a cell can be determined with surprising accuracy (with errors well below 10^{-6}). The specific challenge addressed in this paper lies in a dedicated filtering and validation of the DCI (Downlink Control Information). In a subsequent step the data rates to be expected can be estimated in order to enable decision about the choice of network and the timing of the data offloading to the cloud. The proposed methods have been implemented and validated leveraging the SDR OpenAirInterface, a real-life LTE network and a distributed load generator producing a scalable network traffic by a number of LTE User Equipment.**

I. Introduction

Forecasting the expected data rate of an LTE connection might be useful in many cases. For example, resource constrained Cyber-Physical Systems could decide whether it is worthwhile to offload certain computations to a cloud service or to process them locally, if offloading would require more energy or time. Moreover, this information would enable vehicles to select the currently fastest link for transmitting telemetry data or emergency messages, which might not always be the mobile network but a locally available WiFi hotspot or a Car-to-Car link. Especially warnings about an upcoming hidden tail of a motorway traffic jam might be delayed by the high load of the local LTE cells as a consequence of the high density of devices in this place.

Current LTE networks do not provide any passive indicators to reliably estimate the data rate for an ongoing transmission. Commercial off-the-shelf User Equipment (UE) can only obtain a data rate retrospectively after an actual transmission. Existing indicators like Received Signal Strength Indicator (RSSI), Reference Signal Received Power (RSRP) and Reference Signal Received Quality (RSRQ) allow for a rating of the current radio conditions and therefore an estimation of the highest achievable data rate. But this estimation suffers of large uncertainties as the true data rate highly depends on the current load of the associated evolved NodeB (eNodeB).

As LTE organizes resources in terms of Resource Blocks (RBs) in a resource grid with every RB consisting of mostly 7 symbols and 12 subcarriers, one could measure the signal power on each RB and obtain the utilization. This approach allows the identification of a slightly loaded cell with the expectation of a high data rate for an ongoing transmission as there still remain unused resources (see first column in Fig. 1). However, in case of a fully loaded cell the number of assigned resources highly depends on the total number of active participants (see second and third column in Fig. 1). With this approach that information stays ambiguous, as illustrated in the first row, because the participants cannot be distinguished from signal power in downlink and uplink utilization might be affected by hidden stations that cannot be perceived by the particular UE.

In an LTE network, the assignment of the resources for each UE, designated as Downlink Control Information (DCI), is carried in the Physical Downlink Control Channel (PDCCH) at the beginning of each subframe every 1 ms. Unfortunately,

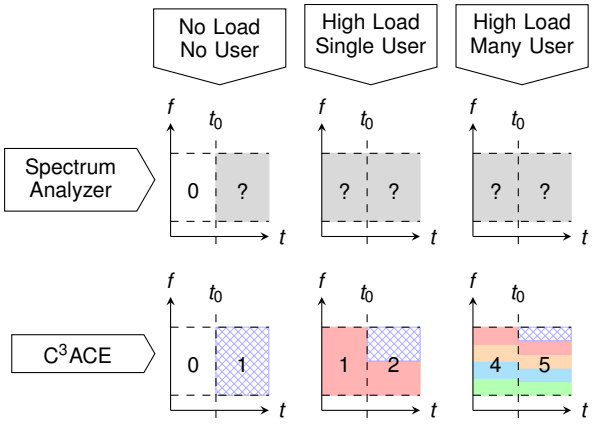

Fig. 1. Simplified illustration of resource occupations when an UE starts a transmission at time t_0 for different cell load scenarios. The granted number of RBs for that UE (crosshatched in blue) depends on the cell load and the number of concurrently transferring UEs. The number of active UEs is unknown at UE side and cannot be derived from signal power using a spectrum analyzer. C^{3}ACE uncovers this number at UE side including the particular allocations of each active participant.

the PDCCH is designed in a way that a UE can only decode its own allocations and common allocations containing public data, e.g. system information.

In this paper we present a Client-based Control Channel Analysis for Connectivity Estimation (C^{3}ACE), a method to decode and process the entire PDCCH obtaining the number of active UEs and the individual resource allocations for both downlink and uplink. We implemented our approach using an open source Software Defined Radio (SDR) UE allowing for real-time passive probing. Furthermore, we show that a joining UE can reliably estimate its expected data rate based on the disclosed information.

II. Related Work

For the evaluation of the current performance of mobile communication system, often active probing mechanisms are applied [1]. For doing so, an active network connection and dedicated network load are required in order to evaluate the performance. In contrast to that, the analysis of passive indicators does not need this dedicated network connection. However, the analysis of passive indicators like the RSRP and RSRQ provide only a stochastic answer about the correlation between indicator and data rate [2]. Further measurement-based analyses (in public LTE networks) of the correlation between passive performance indicators (e.g., RSSI) and LTE data rate are presented in [3]. In order to enhance the forecast quality of the data rate, several approaches that analyze the spectrum can be found in the literature. A performance analysis of 2G mobile networks based on a crowdsourced examination of control traffic by a set of modified smartphones is presented in [4]. In [5] the LTE radio performance is analyzed to discover an inefficient spectrum utilization. For this purpose, the users are localized within a cell. However, the localization requires a rotating antenna to create a Synthetic Aperture Radar (SAR). In addition, this approach does not support a real-time analysis, since a file is periodically written and the results are analyzed offline. An extension of that system can be found in [6]. They provide an adaptive Hypertext Transfer Protocol (HTTP) video streaming over LTE. In order to decrease the risk of stalling video, the base stations' resource allocation is monitored to get information about the available bandwidth. Although this is a real-time implementation, it is not possible to capture the number of active users because only the RB allocation based on the signal power within RBs is analyzed. In contrast to that, we will show is this paper that this value is important for a reliable estimation and we can make it available. The knowledge of the cell occupancy and the number of active users can be leveraged for example to improve the resource efficiency of LTE Machine-Type Communication (MTC) data transmissions in vehicular environments [7] that consider the approximation of the mobile connectivity in the UE.

III. Resource Partitioning in LTE

In LTE the available radio resources, referred as RBs, are shared among active participants and are allocated by the eNodeB. This may happen in different ways, heading for distinct objectives. The eNodeB might share the radio resources in a manner that all active UEs achieve equal data rates. Although this approach seems fair, it has one main disadvantage if few far-distant UEs demand for high data rates. These participants can only reach lower data rates as a consequence of more robust Modulation and Coding Scheme (MCS). This limits the data rates of nearer UEs in a significant way compared to their highest achievable rate. As a result this would lower the User Experience counteracting marketing promises of high data rates made by the network operators.

Another scheduling strategy is to share the available RBs equally or with respect to a particular priority class over the demanding UEs. In case of similar priorities this leads to high data rates for UEs near to the eNodeB and moderate rates for edge UEs at low cell loads. This kind of resource fair scheduling is utilized by the eNodeB of our dedicated network which we will describe later in section V.

In a fully loaded cell with N UEs of equal priority and the aforementioned scheduling the number of RBs allocated to each UE can be estimated by

$$\mathrm{NRB}_{\mathrm{UE}} = \frac{1}{N} \cdot \mathrm{NRB}_{\mathrm{Total}} \tag{1}$$

where $\mathrm{NRB}_{\mathrm{Total}}$ is the eNodeB's total number of available RBs per slot. This results in a data rate

$$r_{\mathrm{UE}} = \mathrm{NRB}_{\mathrm{UE}} \cdot r_0(\mathrm{MCS}_{\mathrm{UE}}) \tag{2}$$

where $r_0(\mathrm{MCS}_{\mathrm{UE}})$ stands for the achievable rate through a single RB at given MCS. Based on this an idle UE can estimate its expected data rate as

$$r_{\mathrm{UE}}^{\mathrm{expected}} = \frac{1}{N+1} \cdot \mathrm{NRB}_{\mathrm{Total}} \cdot r_0(\mathrm{MCS}_{\mathrm{UE}}). \tag{3}$$

While $\mathrm{NRB}_{\mathrm{Total}}$ is known by the UE and the MCS can be derived from already existing connectivity indicators like RSRP and RSRQ at the UE side, the number of active participants is only known by the eNodeB. However, we present that N can be determined by analyzing the eNodeB's PDCCH, requiring modifications of the UE's decoding procedure.

IV. Downlink Control Channel Analysis

The proposed C^{3}ACE approach requires several modifications and additional validation steps within the UE's control channel decoding procedure. To understand the upcoming challenges we first introduce the structure of the PDCCH and the containing data. Afterwards we briefly present the utilized software and hardware platform in which we implemented a passive probe. Finally we focus on the validation of the decoded data which is the crucial part of C^{3}ACE.

A. Structure of the Channel

The PDCCH bears information about the allocation of uplink and downlink resources for particular UEs as well as for common system information about the cell. It is transmitted every 1 ms allocating the RBs of the following LTE subframe. Fig. 2 illustrates the structure of the channel which is divided in a set of Control Channel Elements (CCEs) containing

the actual resource allocations. To obtain a higher degree of robustness against transmission errors the eNodeB may aggregate 1, 2, 4, or 8 consecutive CCEs for one chunk of information using a higher code rate. Furthermore, each chunk contains a Cyclic Redundancy Check (CRC) allowing an integrity check for the received data. This CRC is additionally scrambled with the Radio Network Temporary Identifier (RNTI) of the UE to which it is addressed to.

A usual UE obtains its allocation as follows: After attaching to the eNodeB and receiving its specific RNTI over an encrypted channel, the UE continuously decodes single CCEs and compares the resulting checksum to its assigned RNTI. In case of no match, or if the UE expects further information, it repeats this procedure decoding two consecutive CCEs at once. This is also done for 4 and 8 aggregated CCEs.

Without the knowledge of valid RNTIs a receiver cannot validate the integrity of the decoded chunk. Furthermore, every decoding process at all aggregation levels results in a possibly random sequence of bits as a consequence of noise or a mismatching aggregation (cf. red entries in Fig. 2).

In addition, the actual information carried by CCEs can consist of data structures with different lengths as a result of different DCI formats [8]. These formats serve specific purposes, e.g., compact scheduling or multi-user MIMO scheduling. They are normalized by the eNodeB using rate adaption to fit into whole CCEs thus making them indistinguishable on the channel and demanding the UE for a *trial and error* decoding for all possible formats.

B. Implementation Platform

The proposed passive probe is based on OPENAIRINTERFACE's (OAI) [9] application LTE-SOFTMODEM, an open source SDR implementation of eNodeB and UE. It supports several radio front ends, including the Ettus USRP B210 platform, which we chose.

In order to build our probe, we modified the UE to keep synchronized to a specified eNodeB without making any active access (e.g. attach requests) and to continuously decode the whole PDCCH. The results of the analysis are logged to a file and printed on the screen in real time.

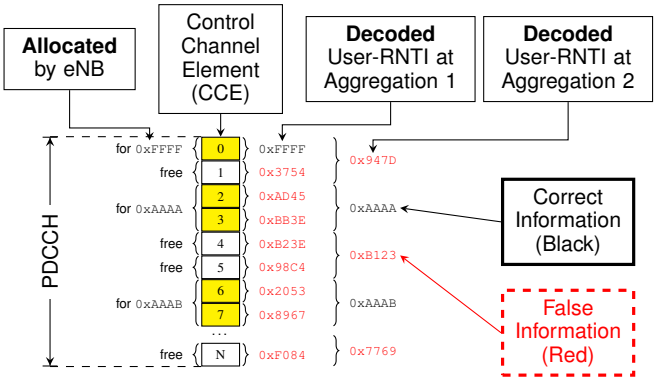

Fig. 2. Structure of the Physical Downlink Control Channel (PDCCH), consisting of numerous CCEs. The eNodeB may place control information at different aggregation levels and leave some CCEs unused forcing the receiver to scan the entire PDCCH at all aggregation levels. Without the knowledge of any valid RNTIs this results in a huge number of invalid information (red).

C. DCI validation

As each DCI's checksum is scrambled with the RNTI to which it is addressed, the probe cannot validate the integrity of the DCI without the knowledge of valid RNTIs (cf. Fig 2). Furthermore, the probe will receive a random bit sequence when decoding unused CCEs, mismatching aggregation levels, and incorrect DCI formats as explained in section IV-A. Hence, the blind analysis will result in a high number of possible DCI with the majority containing invalid information.

In order to remove these invalid DCI we applied a two-step filtering: First we removed impossible DCI, as the eNodeB may place a DCI only in a specific subset of CCEs depending on the current subframe index $(0 \ldots 9)$ and the RNTI it is addressed to [8]. This feature is designed to reduce the search complexity for a normal UE by approximately a fifth in a 10 MHz cell and a tenth in a 20 MHz cell. In our approach we use it to disqualify 80% at 10 MHz and 90% at 20 MHz of received DCI without dropping any valid information.

In the second step we removed all DCI with a high likelihood of containing false information. At this step we evaluated two different approaches of rating the likelihood. The first method was inspired by [5] where each decoded information is being convolutionally re-encoded and compared to the initially received encoded sequence. If the sequences differ by more than few bits, the information is rated as false. Our experiments showed a reliable classification with a threshold of two bit errors per CCE under optimal radio conditions, placing the receiver next to our dedicated eNodeB. Under normal conditions, which is the synchronization to a public eNodeB out of our office, a minimum threshold of about twelve bit errors per CCE was required to classify any valid DCI[1]. With this threshold we observed at least one double-allocation collision of a resource block per subframe, which results in processing false DCI.

In the second approach we first determine valid RNTIs out of the entire value range of possible candidates. For this we assume true RNTIs appear more frequently in the recent period of time while false RNTIs appear equally spread over the value range. The distinction is made by maintaining a histogram of the last n occurred RNTIs and classifying as true those RNTIs which exceed a threshold value k in the histogram.

A snapshot of such a histogram is shown in Fig. 3 during the load analysis of a public cell. It clearly shows certain RNTIs appear more often as a consequence of the dedicated transmissions while arbitrary RNTIs are uniformly distributed, turning up as noise. Moreover, the figure clarifies that the delay for detecting a true positive and the probability for a false positive depend on the chosen threshold value k: A too low threshold will result in a quick true positive detection but also in a high amount of false positive classifications and vice versa.

[1]We evaluated this by exclusively decoding periodic system information having a dedicated RNTI of `0xFFFF`.

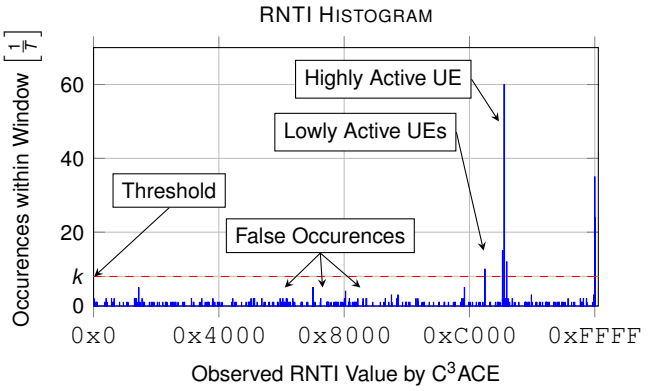

Fig. 3. Snapshot of an RNTI histogram while analyzing the load on a public cell. Active UEs clearly appear as RNTIs with a high number of recent occurrences. False RNTIs are uniformly spread over the value range allowing for a threshold-based filtering.

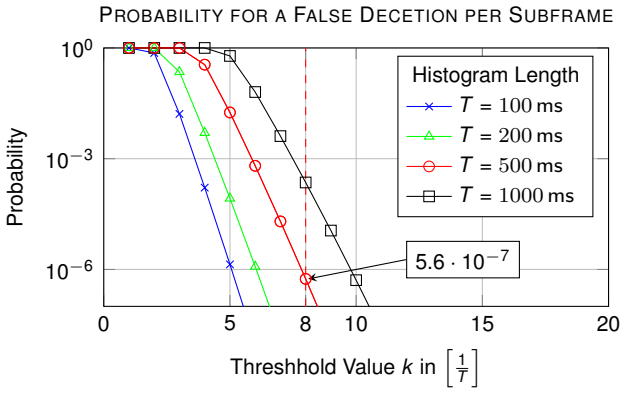

Fig. 4. Probability for a classification error during the analysis of a subframe as function of the chosen threshold value k for various histogram lengths. In case of 500 ms a threshold value $k = 8$ leads to an error probability of $5.6 \cdot 10^{-7}$ for a false detection of any arbitrary RNTI per subframe.

In order to determine the probability for a false positive classification we assume a uniform distribution of false RNTIs. The probability for a particular RNTI $= x$ to result from the decoding of an empty or otherwise used CCE is

$$P(\text{RNTI} = x) = \frac{1}{2^{16}} = p \tag{4}$$

as a fact of 2^{16} possible RNTIs. Within a histogram over n recent RNTIs the probability for a single RNTI value to appear less or equally than k times is

$$P(Z \leq k) = \sum_{i=0}^{k} \binom{n}{i} \cdot p^i \cdot (1-p)^{n-i} \tag{5}$$

which follows from the Bernoulli distribution of n coin tosses. As the calculation of binomial coefficients quickly tends to deal with very large numbers, the probability can be approximated by the Poisson limit theorem [10] for large n and small p as follows:

$$\binom{n}{k} \cdot p^k \cdot (1-p)^{n-k} \simeq e^{-np} \frac{(np)^k}{k!} \tag{6}$$

which leads to

$$P(Z \leq k) \simeq e^{-np} \sum_{i=0}^{k} \frac{(np)^i}{i!}. \tag{7}$$

Finally, the probability for all 2^{16} possible RNTI values to occur k or less times within a histogram is

$$P_{\text{all}}(Z \leq k) = P(Z \leq k)^{(2^{16})}. \tag{8}$$

In order to identify a reliable threshold value k we calculated $P_{\text{all}}(Z \leq k)$ for different histogram lengths as shown in Fig. 4. The corresponding time interval t in seconds covered by the respective histogram is

$$t = \frac{1}{1000} \cdot N_{\text{RNTIs\_per\_subframe}} \cdot p_{\text{Filter1}} \tag{9}$$

where $N_{\text{RNTIs\_per\_subframe}}$ is the number of upcoming RNTI candidates per subframe and p_{Filter1} the filtering rate by the first RNTI-filtering stage described at the beginning of section IV-C. In case of a 10 MHz cell and scanning for DCI formats 0, 1, and 1A [11] these values are typically

$$N_{\text{RNTIs\_per\_subframe}} = 164, \qquad p_{\text{Filter1}} = \frac{1}{5}, \tag{10}$$

which we used in Fig. 4. It shows that the probability for an error-free subframe, without any false positive RNTI, quickly converges to 1. A threshold of $k = 8$ with a histogram length of $t = 500\,\text{ms}$ leads to a probability of $5.6 \cdot 10^{-7}$ for a false positive detection of any RNTI per subframe. Consequently any new upcoming UEs will be detected with a delay of $k = 8$ occurrences which is 8 ms if its RNTI appears once in eight consecutive subframes. While keeping the probability for an error at the same level, the latency might be lowered by reducing the histogram length which consequently lowers the required threshold. A shorter histogram on the other hand leads to a lower recognition rate of sporadically active UEs as their frequency of occurrence may not suffice to exceed the threshold. For our measurements we chose $t = 500\,\text{ms}$ and $k = 8$.

TABLE I
Properties of the Dedicated LTE Test Network

Frequency Band	2.6 GHz (Band 7)
EIRP	158 mW (22 dBm)
Bandwidth	10 MHz (50 RBs)
Duplex Mode	Frequency Division Duplex

V. Measurements

In order to show the benefits of C³ACE, we performed data rate estimations based on the discovered number of active UEs in a cell.

A. Measurement Setup

For our measurements, we used a dedicated LTE network with a configuration as listed in Tab. I. Due to our research license in the chosen frequency band no other interfering networks were in range. Fig. 5 shows a photo of the setup

Fig. 5. Left: Measurement setup of the *near* scenario using an USRP N210 as eNodeB and six STGs including the DUT. Right: LTE passive probe consisting of an USRP B210 and a compact PC executing the modified OAI-software.

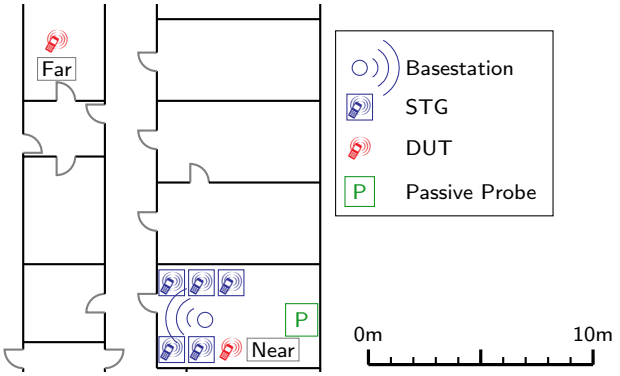

Fig. 6. Overview of the measurement setups for *near* and *far* scenario in our office environment. The corresponding radio conditions are listed in Tab. II.

consisting of an eNodeB, several UEs denoted as Smart Traffic Generators (STGs) [12] including a Device Under Test (DUT), and the passive probe which continuously analyses the PDCCH. The STGs, consisting of an embedded computer and an LTE modem, are used to induce selected traffic load into the cell. As the implementation of the OPENAIRINTERFACE's UE was not fully completed during this work, we switched to a dedicated DUT which is synchronized to the passive probe. The eNodeB is a commercial SDR implementation by Amarisoft using an USRP N210 as radio head.

For a measurement we instructed up to five STGs to transmit as much data as possible in one direction utilizing IPERF3 [13]. Then the passive probe logged the detected number of currently active users to a file emulating an UE evaluating its connectivity for its upcoming transmission. Afterwards the DUT initiated an additional IPERF3-transmission logging the actually achieved data rate. We performed this measurement for a varying number of active STGs, and for poor and good radio conditions by placing the DUT far away or next to the eNodeB as shown in Fig 6. The corresponding connectivity indicators of the DUT are listed in Tab. II. Each single measurement was repeated 50 times.

B. Measurement Results

The achieved uplink data rates of the DUT depending on the detected number of active users by the proposed passive probe are shown in Fig. 7 for both, good and poor radio

TABLE II
RADIO CONDITIONS MEASURED BY THE DUT

Indicator	Near	Far
RSRP	−86 dBm	−129 dBm
RSSI	−65 dBm	−100 dBm
RSRQ	−3	−15

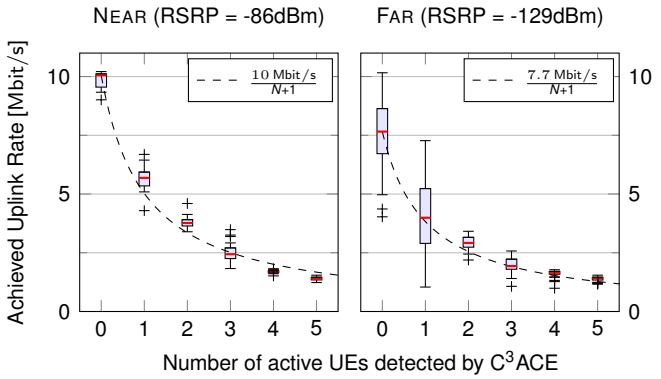

Fig. 7. Achieved uplink data rate of the DUT depending on the detected number of active participants by the passive probe in the moment just before the DUT initiated the transmission. The dashed line shows the expected data rate according to Eq. 3.

conditions, titled as near and far. In addition, the estimated data rate according to a resource fair scheduling (cf. Eq. 3) is plotted as dashed graph. Due to space limitations and greater clarity, we omitted the results for downlink data rates as they showed similar behaviors.

To highlight the estimation error, the difference between estimated and achieved data rate is plotted in Fig. 8. It shows that the error never exceeds 1.7 Mbit/s during our measurements at good radio conditions. Evaluating the cumulative distribution function of the estimation error in Fig. 9 shows that 90% of estimations based on C^{3}ACE have a lower or equal error than 0.7 Mbit/s at good radio conditions. At greater distances the connection suffers of higher packet loss rates and re-

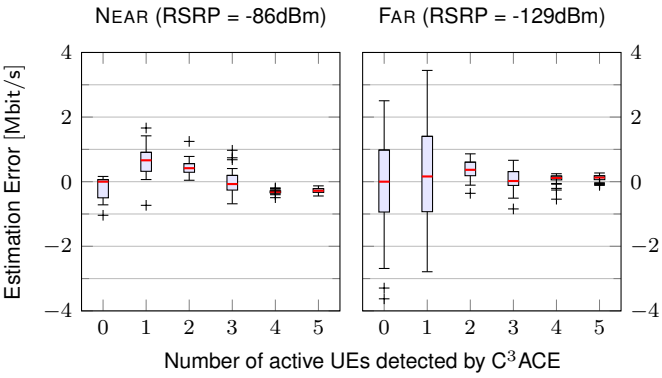

Fig. 8. Corresponding estimation error from expected data rate (c.f. Fig. 7). It shows that the expected data rate for an UE can be derived from the now available number of active UEs with high accuracy. Poor radio conditions result in a higher error variance.

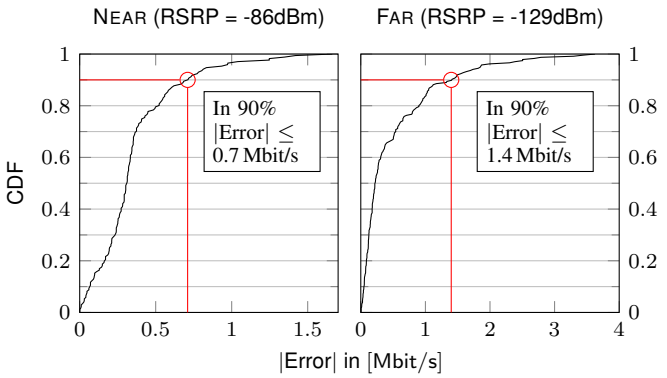

Fig. 9. Cumulative distribution function of the error shown in Fig. 8. At good radio conditions 90% of estimations have an error smaller or equal than 0.7 Mbit/s.

transmissions as a result of the poorer radio link and lead to a larger error deviation. As each participant uses a Transmission Control Protocol (TCP) stream for its transmission, the particular TCP congestion control significantly reduces its data rate in case of packet losses. This spares other UEs additional resources and results in an oscillating data rate. With a larger number of concurring streams, this effect decreases. Still, even in those cases, the estimation stays accurate in average (cf. median in the right chart of Fig. 8) by having an error of less or equal than 1.4 Mbit/s in 90% of estimations.

VI. Conclusion

In this paper we proposed a Client-based Control Channel Analysis for Connectivity Estimation (C^3ACE) technique that enables an UE for a passive determination of the number of active participants within an LTE cell, although an LTE network is not designated to provide this information to an UE. Based on this significant information, and with the knowledge of the eNodeB's scheduling algorithm, the UE can estimate at any moment its expected data rate for an upcoming down- and uplink transmission without the need of active probing. We implemented C^3ACE into an open source SDR UE turning it into a passive probe which is capable of decoding the entire Physical Downlink Control Channel (PDCCH) in real-time. This uncovers the total resource allocations broken down by individual participants. The crux of the matter is a reliable validation of blind decoded control information without the knowledge of any assigned UE-identifier (RNTI) which prevents a checksum verification. We solved this by a histogram-based validation technique, which allows for an adjustable reliability. This approach has a low computational complexity and therefore allows for an efficient integration into future commercial UE.

Afterwards, we performed measurements to evaluate the quality of data rate estimation based on the detected number of active UEs within the cell. The promising results depict an estimation error of less or equal than 0.7 Mbit/s in 90% of cases at good radio conditions within a 10 MHz cell.

Furthermore, the results bring forward the argument that future mobile networks should implement an indicator for the maximum number of currently assignable resources to an UE especially for energy and resource constrained Cyber-Physical Systems. From this, together with the individual radio conditions and the capabilities of the UE (i.e. multiple antennas), the mobile system could accurately evaluate its expected data rate and decide whether to offload data to the cloud or to perform the necessary computations locally.

In future works we will extend our data rate estimation to be independent of the eNodeB's scheduler in consideration of the individual resource demands by active UEs.

Acknowledgment

Part of the work on this paper has been supported by Deutsche Forschungsgemeinschaft (DFG) within the Collaborative Research Center SFB 876 "Providing Information by Resource-Constrained Analysis", project A4.

References

[1] J. Huang, F. Qian, Y. Guo, Y. Zhou, Q. Xu, Z. M. Mao, S. Sen, and O. Spatscheck, "An in-depth study of lte: Effect of network protocol and application behavior on performance," in *Proceedings of the ACM SIGCOMM 2013 Conference on SIGCOMM*, ser. SIGCOMM '13. New York, NY, USA: ACM, 2013, pp. 363–374.

[2] C. Ide, R. Falkenberg, D. Kaulbars, and C. Wietfeld, "Empirical analysis of the impact of lte downlink channel indicators on the uplink connectivity," in *IEEE Vehicular Technology Conference (VTC-Spring)*. Nanjing, China: IEEE, may 2016, accepted for presentation.

[3] C.-P. Wu and K. R. Baker, "Comparison of LTE Performance Indicators and Throughput in Indoor and Outdoor Scenarios at 700 MHz," in *Proc. of IEEE Vehicular Technology Conference*, Quebec City, Canada, Sep. 2012.

[4] A. Achtzehn, J. Riihihjärvi, I. A. Barriía Castillo, M. Petrova, and P. Mähönen, "Crowdrem: Harnessing the power of the mobile crowd for flexible wireless network monitoring," in *Proceedings of the 16th International Workshop on Mobile Computing Systems and Applications*, ser. HotMobile '15. New York, NY, USA: ACM, 2015, pp. 63–68.

[5] S. Kumar, E. Hamed, D. Katabi, and L. Erran Li, "Lte radio analytics made easy and accessible," in *Proceedings of the 2014 ACM Conference on SIGCOMM*, ser. SIGCOMM '14. New York, NY, USA: ACM, 2014, pp. 211–222.

[6] X. Xie, X. Zhang, S. Kumar, and L. E. Li, "pistream: Physical layer informed adaptive video streaming over lte," in *Proceedings of the 21st Annual International Conference on Mobile Computing and Networking*, ser. MobiCom '15. New York, NY, USA: ACM, 2015, pp. 413–425.

[7] C. Ide, B. Dusza, and C. Wietfeld, "Client-based Control of the Interdependence between LTE MTC and Human Data Traffic in Vehicular Environments," *IEEE Transactions on Vehicular Technology*, vol. 64, no. 5, pp. 1856–1871, May 2015.

[8] *3GPP TS 36.213 - Physical layer procedures (Release 13)*, 3rd Generation Partnership Project Technical Specification, Rev. V13.0.1, Jan. 2016. [Online]. Available: http://www.3gpp.org/ftp/specs/archive/36_series/36.213/

[9] OpenAirInterface Software Alliance, "Open Air Interface," 2016. [Online]. Available: http://www.openairinterface.org/

[10] A. Papoulis, *Probability, Random Variables, and Stochastic Processes*, 4th ed., ser. McGraw-Hill series in electrical engineering. New York: McGraw-Hill, 2002.

[11] *3GPP TS 36.212 - Multiplexing and channel coding (Release 13)*, 3rd Generation Partnership Project Technical Specification, Rev. V13.0.0, Dec. 2015. [Online]. Available: http://www.3gpp.org/ftp/specs/archive/36_series/36.212/

[12] D. Kaulbars, F. Schweikowski, and C. Wietfeld, "Spatially distributed traffic generation for stress testing the robustness of mission-critical smart grid communication," in *IEEE GLOBECOM 2015 Workshop on SmartGrid Resilience*, San Diego, USA, Dec. 2015.

[13] J. Dugan, S. Elliott, B. A. Mah, J. Poskanzer, and K. Prabhu, "iPerf3," 2015. [Online]. Available: https://iperf.fr